Comparison of Dual-Tracer PET and CT Features to Conventional Risk Categories in Assessing Response to ^{177}Lu-PSMA-617 Therapy for Metastatic Prostate Adenocarcinoma with Urinary Bladder Involvement

Aadil Adnan and Sandip Basu

Radiation Medicine Centre, Bhabha Atomic Research Centre, Tata Memorial Centre Annexe, and Homi Bhabha National Institute, Mumbai, India

The present communication details the imaging characteristics, peculiarities, and response to ^{177}Lu-labeled prostate-specific membrane antigen (PSMA)-617–targeted radioligand therapy (PRLT) in accordance with Gleason score and use of dual-tracer PET (^{68}Ga-PSMA-11 and ^{18}F-FDG) in patients with urinary bladder invasion or metastasis by prostate cancer, including the prognostic value of ^{18}F-FDG PET in predicting response to treatment. The CT attenuation units (Hounsfield units) correlated with the prostate primary in the case of direct tumor extension from the prostate, whereas in hematogenous metastatic seeding the Hounsfield units were lower than in the primary prostatic tumor. A favorable outcome to ^{177}Lu-PSMA-617 PRLT was observed in patients with low or no baseline ^{18}F-FDG uptake despite a high Gleason score and a high-risk National Comprehensive Cancer Network prognostic category and did not correlate with the latter alone, whereas a high SUV_{max} on ^{18}F-FDG PET/CT was associated with an adverse outcome. These findings suggest a promising role for ^{18}F-FDG PET/CT in predicting therapeutic outcomes more confidently, and hence the concept of dual-tracer PET appears to hold good in prostate adenocarcinoma theranostics.

Key Words: metastatic prostate adenocarcinoma; mCRPC; ^{68}Ga-PSMA-11 PET/CT; ^{18}F-FDG PET/CT; ^{177}Lu-PSMA-617; peptide receptor radioligand therapy

J Nucl Med Technol 2020; 48:148–153
DOI: 10.2967/jnmt.119.235960

Prostate carcinoma is the second most frequently diagnosed cancer and the sixth leading cause of cancer-related death in men worldwide (*1*). About 20% of the patients have metastatic disease, with common sites being pelvic and abdominal nodes, urinary bladder (direct infiltration > hematogenous seeding), and skeleton (axial > appendicular skeleton) (*1*). On the other hand, the most common tumor involving the urinary bladder is primary urothelial carcinoma (*2*). Secondary urinary bladder tumors are relatively uncommon and account for about 2%–13% of all tumors, most being due to a primary in the prostate or adjacent organs (*2,3*). Urinary bladder metastases from prostatic adenocarcinoma can occur in 2 ways: direct extension of the prostatic tumor and multifocal, exophytic hematogenous seeding (mimicking multifocal primary urothelial carcinoma). The former is more common and involves mainly the bladder neck and trigone, whereas the latter is mostly multifocal and usually involves muscle wall rather than being intravesicular.

Presently, the mainstays of imaging are MRI and multiparametric MRI for prostate adenocarcinoma and CT and MRI for urothelial carcinoma of the urinary bladder (*4*). These imaging modalities, however, have limited capabilities in detecting subcentimetric disease, particularly nodal metastases. Of late, there has been remarkable improvement in molecularly targeted imaging with the advent of newer PET tracers in clinical practice for prostate carcinoma. One of the most important and widely used tracers is directed toward prostate-specific membrane antigen (PSMA), which is abundantly expressed on prostatic tumors, particularly in castration-resistant cases, and on the neovasculature of several solid tumors (*5,6*). Targeting PSMA for imaging dates back to 2006–2007, when radiolabeled J591 antibodies were used for γ-camera–based planar scans (*7*). More recently, urea-based, gallium-labeled small-molecule inhibitors of PSMA, known as PSMA-11 or PSMA-HBED-CC, have been widely used along with other novel tracers such as fluorine-labeled PSMA-DCFPyL or PSMA-1007 for PET imaging and ^{177}Lu-labeled PSMA-617 for PSMA-targeted radioligand therapy (PRLT) (*8–12*).

Herein, we present data from a series of 3 patients diagnosed as having prostatic adenocarcinoma metastasizing to the urinary bladder with different histopathologic patterns and Gleason grades, treated with ^{177}Lu-PSMA-617 PRLT. The

Received Aug. 31, 2019; revision accepted Oct. 31, 2019.
For correspondence or reprints contact: Sandip Basu, Radiation Medicine Centre, Bhabha Atomic Research Centre, Tata Memorial Hospital Annexe, Jerbai Wadia Rd., Parel, Mumbai, Maharashtra, India 400 012.
E-mail: drsanb@yahoo.com
Published online Feb. 28, 2020.

presented cases are complemented by a table (Table 1) summarizing key patient characteristics and imaging features on ^{68}Ga-PSMA-11 and ^{18}F-FDG PET/CT before and after ^{177}Lu-PSMA-617. The primary intent was to study the various imaging characteristics (both molecular and anatomic) of metastatic urinary bladder lesions secondary to prostatic adenocarcinoma. We have also tried to bring attention to the role of baseline ^{18}F-FDG PET/CT in disease prognostication and prediction of long-term outcome, particularly after PRLT.

CASE 1

A 65-y-old man, known to be diabetic and hypertensive, on medical management presented with lower-urinary-tract symptoms of 6-mo duration with an episode of acute urinary retention. Further evaluation showed grade I prostatomegaly and a raised serum level of prostate-specific antigen (PSA) (58.18 ng/mL). Transrectal ultrasound-guided biopsy showed poorly differentiated adenocarcinoma, Gleason score 4 + 4. Metastatic workup showed locally invasive and distant metastatic disease. He received hormonal therapy followed by bilateral orchidectomy and chemotherapy. After chemotherapy, he presented with a rising PSA with new-onset left-shoulder pain and was started on abiraterone and prednisolone. Follow-up showed a rising PSA and disease progression, and he was referred for ^{177}Lu-PSMA therapy. ^{18}F-FDG PET/CT as part of the pretherapy workup showed no significant uptake in the prostatic or sacral lesions, with mild to moderate hypermetabolism in the sclerotic lesion in the left humerus. He received 1 cycle of ^{177}Lu-PSMA-617. At follow-up, he reported complete relief from shoulder pain, and there was some reduction in PSA level (from 65.128 to 33.062 ng/mL).

A comparative analysis of ^{68}Ga-PSMA-11 and ^{18}F-FDG PET/CT at baseline and after the first cycle of ^{177}Lu-PSMA-617 therapy is given in Figure 1 and Table 1. PSMA expression increased in the right lobe of the prostate, with infiltration into the urinary bladder along with increased PSMA expression in sclerotic lesions involving the left humerus and sacrum. ^{18}F-FDG PET/CT at baseline showed no significant metabolism in the prostatic lesion, with low-grade metabolic activity in left humeral and sacral sclerotic lesions. After the first cycle of ^{177}Lu-PSMA-617 therapy, the size of the prostatic lesion decreased and the intravesical component of tumor infiltration showed a significant reduction in PSMA expression. No significant interval change in metabolic activity was noted in the left humeral or sacral sclerotic lesions. The CT attenuation units (Hounsfield units [HU]) of the urinary bladder metastases showed a reduction from 96 to 67 at this time, whereas those of the prostate decreased from 100 to 70.

CASE 2

The second patient was a 58-y-old man with type 2 diabetes and hypertension on medical management, who had presented in 2010 with hesitancy in passing urine. On evaluation, there was a raised PSA level. Transrectal ultrasound–guided biopsy of the prostate found adenocarcinoma, and the Gleason score was 4 + 3. MRI showed a prostatic lesion with involvement of the seminal vesicles and regional lymph nodes. He underwent bilateral orchiectomy.

TABLE 1
Key Patient Characteristics and Imaging Features

Characteristic	Patient 1	Patient 2	Patient 3
Histopathology	Poorly differentiated adenocarcinoma	Conventional adenocarcinoma	Conventional adenocarcinoma
Gleason score	4 + 4	4 + 3	4 + 5
National Comprehensive Cancer Network prognostic category	High risk	Intermediate risk	High risk
PSA (ng/mL)			
Baseline	65.128	751	228.03
After ^{177}Lu-PSMA	33.062	1,761.25	44.54
^{68}Ga-PSMA-11 uptake (SUV_{max})			
Baseline	64.73	27.04	116.84
After ^{177}Lu-PSMA	28.02	36.65	83.6
^{18}F-FDG uptake (SUV_{max})			
Baseline	8.38	22.88	8.4
After ^{177}Lu-PSMA	4.41	9.63	4.5
Metastatic pattern of urinary bladder	Direct extension from prostate	Direct extension from prostate	Multifocal metastatic lesions involving bladder wall, hematogenous
HU of prostate			
Baseline	100	125	93
After ^{177}Lu-PSMA	70	108	67
HU of urinary bladder metastases			
Baseline	96	116	70
After ^{177}Lu-PSMA	67	83	41
Outcome	Partial response	Progression and death	Partial response

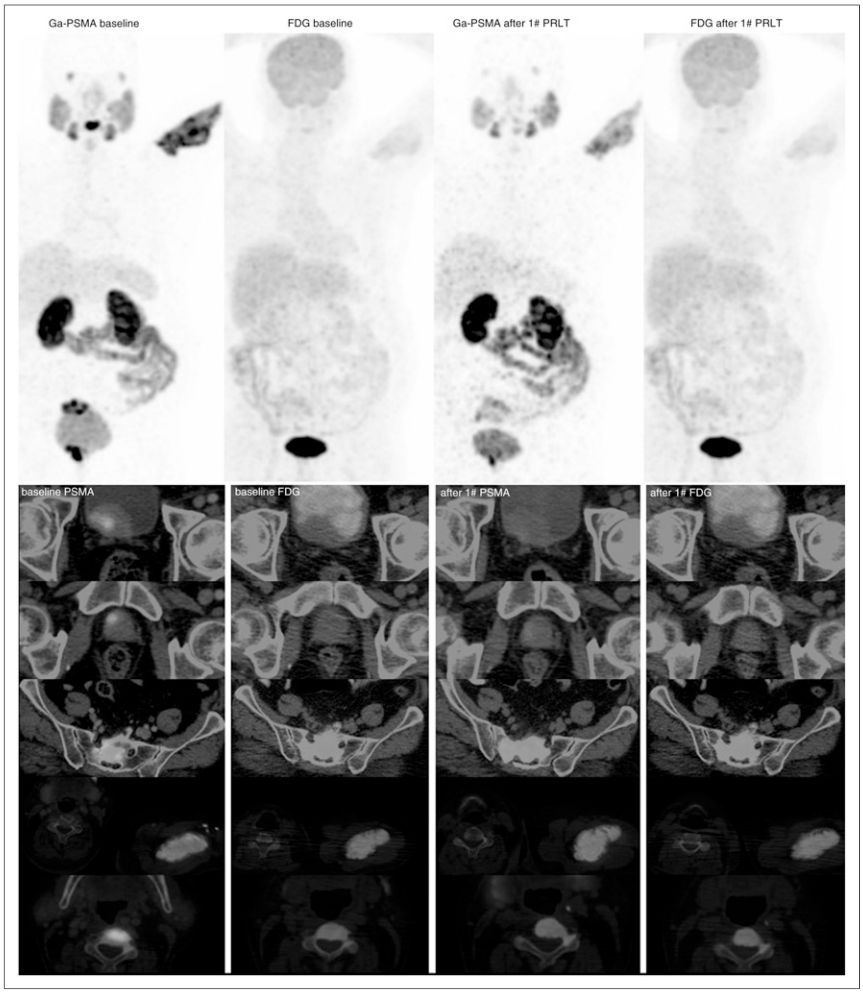

FIGURE 1. Comparative analysis of PSMA and ^{18}F-FDG PET/CT scans at baseline (left 2 panels) and after ^{177}Lu-PSMA PRLT (right 2 panels) for patient 1.

A metastatic workup was negative for metastases. Subsequently, he was started on hormonal therapy (in view of the rising PSA) followed by abiraterone (in view of biochemical progression). At that time, he developed metastatic liver lesions (biopsy-proven) and was started on chemotherapy. After chemotherapy, there was a rising PSA (153 ng/mL). He underwent channel transrectal ultrasound for urinary retention followed by palliative local radiotherapy to the lumbar spine. After radiotherapy, he was started on enzalutamide, which was followed by a rising PSA with new skeletal lesions, and he was advised to begin mitoxantrone. Thereafter, he showed a raised PSA (283 ng/mL) and new skeletal and hepatic lesions on ^{18}F-FDG PET/CT. Restaging ^{68}Ga-PSMA-11 PET/CT revealed disease progression. He was referred for ^{177}Lu-PSMA-617 PRLT.

He received 5 cycles of ^{177}Lu-PSMA-617 therapy (cumulative activity, 23,421 MBq [633 mCi]). Follow-up evaluations after the first cycle suggested good symptomatic relief. However, no significant biochemical response was noted except after the second cycle, when there was some decline in PSA level. During further follow-ups, he presented with anatomic and biochemical progression (PSA, 1,100 ng/mL) (Fig. 2). In view of the disease progression, no further PRLT was planned and he was referred back to the referring unit for further management. He received further hormonal therapy and multiple lines of chemotherapy with some symptomatic and biochemical response (a fall in PSA from a maximum of 6,219 ng/mL to a nadir of 1,761.25 ng/mL). He finally succumbed to his disease. The HU of the urinary bladder metastases decreased from 116 to 93 although the PSMA uptake increased from 27 to 36. The HU of the prostate decreased modestly from 125 to 108.

CASE 3

A 65-y-old man with no comorbidities presented with lower-urinary-tract symptoms of an 8-mo duration. On evaluation, he was found to have a raised PSA (250.383 ng/mL). Further imaging with MRI revealed a large, enhancing lesion arising from the prostate with invasion into the bladder, along with multiple exophytic lesions involving the right lateral and posterior walls of the urinary bladder (biopsy-proven to be metastatic adenocarcinoma). Digital rectal examination showed a large grade III nodular, hard prostate. Transrectal ultrasound–guided biopsy revealed conventional prostatic adenocarcinoma, Gleason score 4 + 5. Metastatic workup revealed lesions suspected of being metastases. ^{18}F-FDG PET/CT showed metabolically active metastatic disease. The patient underwent bilateral orchidectomy and was started on chemotherapy with docetaxel, which induced interstitial lung disease (reversed on steroids). After docetaxel, follow-up was suggestive of a favorable response, with a low serum PSA. This state was maintained for some time, after which the patient experienced a asymptomatic serial rise in serum PSA and was given a docetaxel rechallenge in view of the progression of biochemical (PSA, 42.403 ng/mL) and morphologic disease as reflected on ^{68}Ga-PSMA-11 PET/CT scans. The patient later received abiraterone for 3 mo and was shifted to cyclophosphamide because of biochemical progression (PSA, 183 ng/mL). He received cyclophosphamide for 6 mo, with some biochemical response (PSA, 71 ng/mL), followed by biochemical disease progression (PSA, 228.034 ng/mL).

The details of the dual-tracer PET and CT characteristics of the prostate and urinary bladder lesion are summarized in Table 1. Interestingly, the HU were found to be relatively

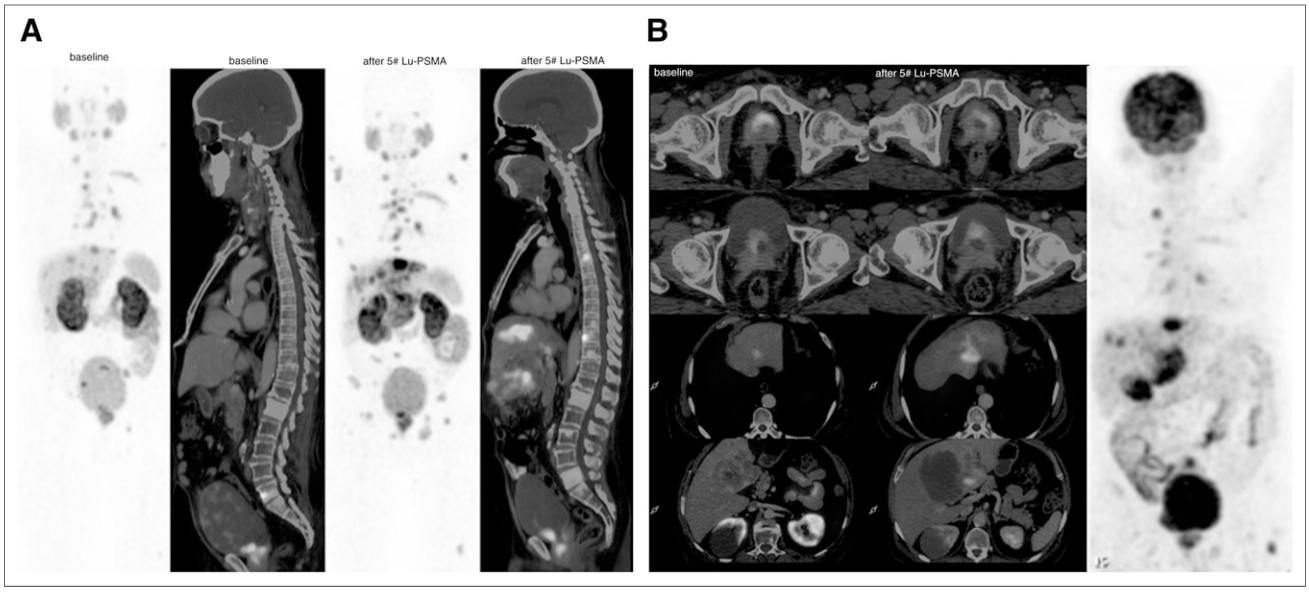

FIGURE 2. (A) Comparative analysis of ^{68}Ga-PSMA-11 PET/CT scans at baseline and after ^{177}Lu-PSMA-617 therapy for patient 2. (B) Maximum-intensity projection of baseline ^{18}F-FDG PET/CT scan.

lower (70 vs. 93) in multifocal noncontiguous bladder wall metastases (likely hematogenous seeding) than in the prostate, unlike cases of direct extension of tumor into the urinary bladder. On follow-up, scans for response evaluation and further treatment planning (Fig. 3) demonstrated, on comparative analysis, a significant decrease in size and PSMA uptake in the prostatic lesion, with a decrease in the number of exophytic vesicular lesions. A significant decrease was noted in the number of abdominal and pelvic nodes and in their PSMA uptake, along with complete resolution of the right hilar lymphadenopathy. ^{18}F-FDG PET/CT at that time showed complete metabolic resolution. These findings correlated well with a good biochemical response (a PSA decrease from 228.03 to 44.54 ng/mL).

DISCUSSION

Urinary bladder involvement by prostate adenocarcinoma occurs late in the course of the disease. Thus, any potential treatment is usually palliative. The symptomatic profile ranges from asymptomatic to dysuria or hematuria. It is important to differentiate metastatic lesions from primary urothelial carcinomas, especially in cases of multifocal bladder lesions, to initiate appropriate therapeutic strategies early. The diagnosis is primarily by histopathologic examination with immunohistochemistry, the latter mainly to differentiate more confidently between urothelial transitional cell carcinoma and adenocarcinoma. The immunohistochemistry markers for prostate carcinoma are PSA, prostatic acid phosphatase, and P504, with negative staining for P63, CK7, CK20, and villin (*13*). MRI forms the mainstay for imaging, followed by transrectal ultrasound and—with limited potential—CT. In prostatic adenocarcinoma, ^{68}Ga-PSMA-11 PET/CT, which shows avid uptake at both primary and metastatic sites, may be a valuable adjunct in making the diagnosis. Urothelial carcinoma usually shows low-grade to no uptake; this could be explained by scant neovascularization and associated low levels of PSMA expression, as is evident from RNA-sequencing data and immunohistochemistry staining (*14*). In the literature, a couple of reports exist on PSMA positivity in urothelial carcinoma (*15,16*).

CT parameters, particularly HU, can give some idea on the pathologic involvement of the prostate. A normal prostate gland is a soft-tissue structure with HU ranging from 40 to 60 in the central zone and 10 to 25 in the peripheral zone (*17*). Higher values of more than 25 HU in the peripheral zone and, especially, equaling those of the central zone are suggestive of pathologic involvement and may even indicate malignancy (*17*). Prognostication in prostate carcinoma depends mainly on the size of the primary tumor (T stage) and on Gleason score and baseline PSA, as per the guidelines of the National Comprehensive Cancer Network and other internationally accepted guidelines, and is divided into low-, intermediate-, and high-risk categories (*18,19*). Avid ^{18}F-FDG uptake on PET/CT in tumors usually reflects aggressiveness and poor long-term prognosis.

In our series, 2 patients had direct extension of the prostatic tumor into the urinary bladder, involving the neck and trigone, whereas the other had multifocal lesions involving the bladder wall. One of the 2 patients with direct tumor extension had high-risk, poorly differentiated adenocarcinoma (patient 1), whereas the other had conventional adenocarcinoma with intermediate risk (patient 2). The third patient, with multifocal bladder wall lesions, had high-risk conventional adenocarcinoma (patient 3). Patient 1 demonstrated avid PSMA and moderate ^{18}F-FDG uptake at baseline and showed a significant decline in PSA level after ^{177}Lu-PSMA-617 therapy,

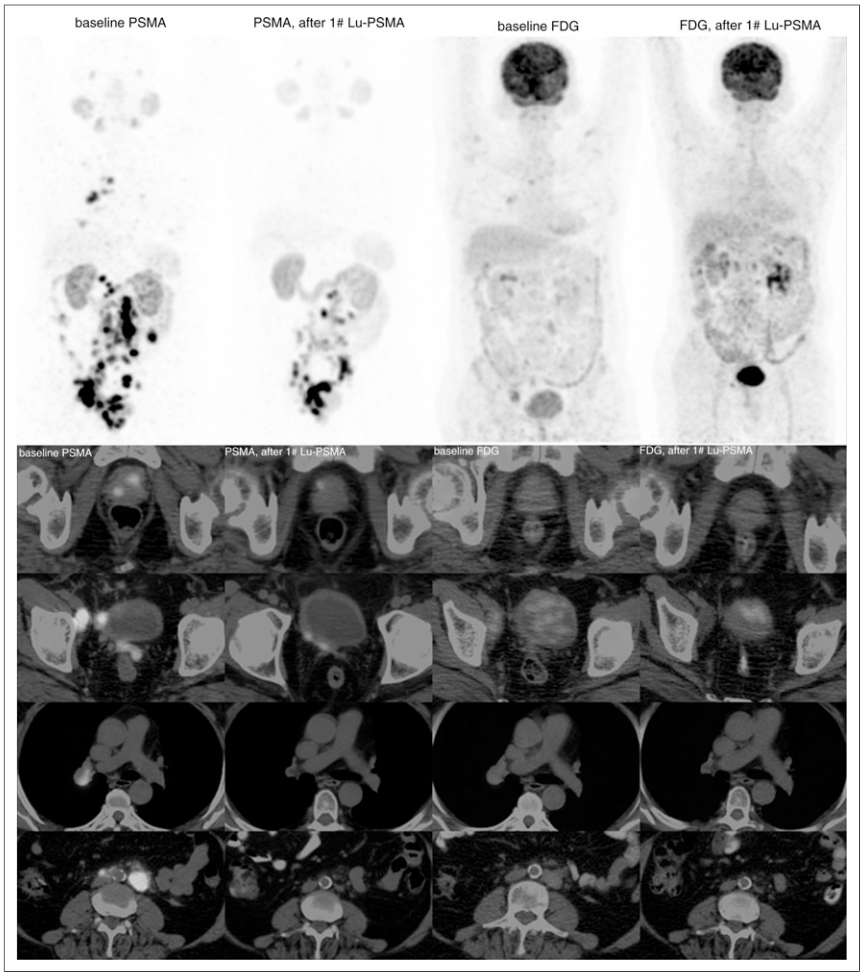

FIGURE 3. Comparative analysis of ^{68}Ga-PSMA-11 PET/CT (left 2 panels) and ^{18}F-FDG PET/CT (right 2 panels) at baseline and after ^{177}Lu-PSMA-617 PRLT for patient 3.

qualifying as a partial response as per RECIST 1.1 and PERCIST 1. Patient 2 demonstrated avid PSMA and high ^{18}F-FDG uptake at baseline and showed a significant (>2-fold) rise in PSA after ^{177}Lu-PSMA-617 therapy, with significant disease progression culminating in death. Interestingly, in both patient 1 and patient 2, with direct extension of the prostatic tumor into the urinary bladder, the HU almost corresponded to those of the prostatic lesion (100 HU and 96 HU in the urinary bladder and prostate lesion, respectively, for patient 1 and 125 HU and 116 HU, respectively, for patient 2). Patient 3, with multifocal urinary bladder wall metastases, demonstrated avid PSMA with moderate ^{18}F-FDG uptake on baseline scans and showed a partial response, with a significant decline (>5-fold) in PSA after ^{177}Lu-PSMA-617 therapy. HU were less than those of the prostatic lesion (93 HU and 70 HU in the prostate and urinary bladder, respectively), as opposed to those observed in the previous 2 patients, who had direct prostatic tumor extension into the urinary bladder. After ^{177}Lu-PSMA-617 therapy, all patients demonstrated a significant decline in PSMA, in ^{18}F-FDG uptake by the lesions, and in HU.

Overall prognosis was associated more closely with ^{18}F-FDG metabolism than with histopathologic differentiation, Gleason score, pretreatment prognostic category, or PSA value. Baseline aggressive tumor biology, reflected by a high SUV_{max} on ^{18}F-FDG PET/CT, was associated with an adverse outcome, suggesting a promising role for ^{18}F-FDG PET/CT in long-term prognostication and prediction of therapeutic outcome. Hence, the concept of dual-tracer PET appears to hold good in prostate adenocarcinoma.

CONCLUSION

Our study illustrates that in patients with longstanding metastatic prostate cancer with multifocal bladder lesions, the possibility of metastatic prostatic adenocarcinoma should be considered. Although the definitive diagnosis is with histopathology and immunohistochemistry, avid uptake on ^{68}Ga-PSMA-11 PET/CT favors a prostatic origin and can be used as a noninvasive diagnostic adjunct to differentiate the two. HU in the urinary bladder correlate with those of the prostate in cases of direct extension of tumor into the urinary bladder and are relatively lower in multifocal bladder wall metastases (hematogenous seeding). Hence, ^{18}F-FDG PET/CT along with ^{68}Ga-PSMA-11 PET/CT, preferably at baseline, can subserve prognostic and predictive implications, particularly for ^{177}Lu-PSMA-617–based PRLT. The intriguing observations made on the 3 patients of this study merit examination in a larger sample.

DISCLOSURE

No potential conflict of interest relevant to this article was reported.

REFERENCES

1. Siddiqui E, Mumtaz FH, Gelister J. Understanding prostate cancer. *J R Soc Promot Health.* 2004;124:219–221.
2. Melicow MM. Tumors of the urinary bladder: a clinicopathological analysis of over 2500 specimens and biopsies. *J Urol.* 1955;74:498–521.
3. Bates AW, Baithun SI. Secondary neoplasms of the bladder are histological mimics of nontransitional cell primary tumours: clinicopathological and histological features of 282 cases. *Histopathology.* 2000;36:32–40.
4. Clark PE, Agarwal N, Biagioli MC, et al. Bladder cancer. *J Natl Compr Canc Netw.* 2013;11:446–475.
5. Chang SS, O'Keefe DS, Bacich DJ, Reuter VE, Heston WD, Gaudin PB. Prostate-specific membrane antigen is produced in tumour associated neovasculature. *Clin Cancer Res.* 1999;5:2674–2681.
6. Chang SS, Reuter VE, Heston WD, Bander NH, Grauer LS, Gaudin PB. Five different anti-prostate-specific membrane antigen (PSMA) antibodies confirm PSMA expression in tumour associated neovasculature. *Cancer Res.* 1999;59:3192–3198.

7. Pandit-Taskar N, O'Donoghue JA, Divgi CR, et al. Indium-111 labeled J591 anti-PSMA antibody for vascular targeted imaging in progressive solid tumors. *EJNMMI Res.* 2015;5:28.
8. Szabo Z, Mena E, Rowe SP, et al. Initial evaluation of [^{18}F]DCFPyL for prostate-specific membrane antigen (PSMA)-targeted PET imaging of prostate cancer. *Mol Imaging Biol.* 2015;17:565–574.
9. Rowe SP, Drzezga A, Neumaier B, et al. Prostate-specific membrane antigen-targeted radiohalogenated PET and therapeutic agents for prostate cancer. *J Nucl Med.* 2016;57(suppl 3):90S–96S.
10. Rowe SP, Gorin MA, Salas Fragomeni RA, Drzezga A, Pomper MG. Clinical experience with ^{18}F-labeled small molecule inhibitors of prostate-specific membrane antigen. *PET Clin.* 2017;12:235–241.
11. Dietlein M, Kobe C, Kuhnert G, et al. Comparison of [^{18}F]DCFPyL and [^{68}Ga] PSMA-HBED-CC for PSMA-PET imaging in patients with relapsed prostate cancer. *Mol Imaging Biol.* 2015;17:575–584.
12. Dietlein F, Kobe C, Neubauer S, et al. PSA-stratified performance of ^{18}F- and ^{68}Ga-PSMA PET in patients with biochemical recurrence of prostate cancer. *J Nucl Med.* 2017;58:947–952.
13. Molinié V, Vieillefond A, Michiels JF. Evaluation of p63 and p504s markers for the diagnosis of prostate cancer. *Ann Pathol.* 2008;28:417–423.
14. Huang TB, Yan Y, Liu H, et al. Metastatic prostate adenocarcinoma posing as urothelial carcinoma of the right ureter: a case report and literature review. *Case Rep Urol.* 2014;2014:230852.
15. Gupta M, Choudhury PS, Gupta G, Gandhi J. Metastasis in urothelial carcinoma mimicking prostate cancer metastasis in Ga-68 prostate-specific membrane antigen positron emission tomography-computed tomography in a case of synchronous malignancy. *Indian J Nucl Med.* 2016;31:222–224.
16. Zacho HD, Pedersen SH, Petersen A, Petersen LJ. ^{68}Ga-PSMA PET/CT uptake in the ureter caused by ligand expression in urothelial cancer. *Clin Nucl Med.* 2020;45:e43–e45.
17. Dhawan S, Gothi R, Aggarwal A, Aggarwal B, Doda SS. Computed tomography in prostatic cancer. *Indian J Radiol Imaging.* 2005;15:199–201.
18. Rodrigues G, Warde P, Pickles T, et al. Pre-treatment risk stratification of prostate cancer patients: a critical review. *Can Urol Assoc J.* 2012;6:121–127.
19. Mohler J, Bahnson RR, Boston B, et al. NCCN clinical practice guidelines in oncology: prostate cancer. *J Natl Compr Canc Netw.* 2010;8:162–200.